Quantum-state engineering assisted by entanglement

Matteo G. A. Paris*
Quantum Optics & Information Group, INFM Unità di Pavia, Pavia, Italy

Mary Cola† and Rodolfo Bonifacio
Dipartimento di Fisica and Unità INFM, Università di Milano, Milano, Italy
(Received 7 November 2002; published 10 April 2003)

We suggest a general scheme for continuous variable quantum-state engineering based on conditional measurements carried out on entangled twin beam of radiation. Realistic detection schemes such as on/off photodetection, homodyne detection, and joint measurement of two-mode quadratures are analyzed in detail. Imperfections of the apparatuses, such as nonunit quantum efficiency and finite resolution, are taken into account. We show that conditional on/off photodetection provides a reliable scheme to verify nonclassicality, whereas conditional homodyning represents a tunable and robust source of squeezed light. We also describe optical continuous variable teleportation as a conditional measurement, and evaluate the degrading effects of finite amount of entanglement, decoherence due to losses, and nonunit quantum efficiency.

DOI: 10.1103/PhysRevA.67.042104 PACS number(s): 03.65.Ud, 03.67.Mn, 42.50.Dv

I. INTRODUCTION

Quantum-state engineering of radiation field plays a major role in several fundamental tests of quantum mechanics [1], as well as in applications such as high-precision measurements and high-capacity communication channels [2]. Generation of nonclassical light generally involves active devices and nonlinear optical media, which couple two or more modes of the field through the nonlinear susceptibility of the matter. Since the nonlinear susceptibilities are small, the effective implementation of nonlinear interactions is experimentally challenging, and the resulting processes are generally characterized by a low rate of success, i.e., by a low efficiency.

In quantum mechanics, the reduction postulate provides an alternative *intrinsic* mechanism to achieve *effective* nonlinear dynamics. In fact, if a measurement is performed on a portion of a composite entangled system, e.g., the bipartite entangled systems made of two modes of radiation, the other component is conditionally *reduced* according to the outcome of the measurement [3]. The resulting dynamics is highly nonlinear, and may produce quantum states that cannot be generated by currently achievable nonlinear processes. The efficiency of the process, i.e., the rate of success in getting a certain state, is equal to the probability of obtaining a certain outcome from the measurement. This is usually higher than nonlinear efficiency, thus making conditional schemes possibly convenient even when a corresponding Hamiltonian process exists.

The nonlinear dynamics induced by conditional measurements has been analyzed for a large variety of tasks [4–18], among which we mention photon adding and subtracting schemes [5], optical state truncation of coherent states [6], generation of catlike (macroscopic quantum interference) states [7–9], state filtering by active cavities [10,11], synthesis of arbitrary unitaries [12], and generation of optical qubit by conditional interferometry [13].

In this paper, we analyze in detail the use of conditional measurements on entangled twin beam of radiation (TWB) to engineer quantum states, i.e., to produce, manipulate, and transmit nonclassical light. In particular, we will focus our attention on realistic measurement schemes, feasible with current technology, and will take into account imperfections of the apparatuses such as detection quantum efficiency and finite resolution.

The reason to choose TWB as an *entangled resource* for conditional measurements is twofold. On one hand, TWBs are the natural generalization to continuous variable (CV) systems of Bell states, i.e., maximally entangled states for qubit systems. On the other hand, and more importantly, TWBs are the only CV entangled states that can be reliably produced with current technology, either by parametric down-conversion of the vacuum in a nondegenerate parametric amplifier [19], or by mixing two squeezed vacua from a couple of degenerate parametric amplifiers in a balanced beam splitter [20,21]. Overall, our main goal is to establish the current state of art for conditional engineering of CV quantum states assisted by entanglement.

The first kind of measurement we analyze is on/off photodetection. As a matter of fact, though recent proposals are encouraging [22], the discrimination of, say, n photons from $n+1$ photons in the quantum regime is still experimentally challenging. Therefore, we are led to consider the action of realistic avalanche on/off photodetectors, i.e., detectors that have no output when no photon is detected and a fixed output when one or more photons are detected. Our analysis shows that on/off photodetection on TWB provides the generation of conditional *nonclassical mixtures*, which are not destroyed by decoherence induced by noise and permits a robust test of the quantum nature of light. The second apparatus involves homodyne detection, whose action on TWB represents a tunable source of squeezed light, with high conditional probability and robustness to experimental imperfections, such as nonunit quantum efficiency and finite resolution. The third

*Electronic address: paris@unipv.it; URL: www.qubit.it/~paris
†Electronic address: mary.cola@mi.infn.it

kind of measurement we are going to consider is the joint measurement of the sum and difference quadratures of two modes corresponding to the measurement of the real and the imaginary parts of the complex photocurrent $Z=a+b^{\dagger}$, a and b being two modes of the field. Such a measurement is realized by generalized heterodyne detection if the two modes have different frequencies, and by multiport homodyne detection if they have the same frequency. In our case, one of the two modes is a beam of the TWB, whereas the second mode is excited in a given reference state, usually referred to as the probe of the measurement. As we will see, this approach allows us to describe CV quantum teleportation as a conditional measurement, and to easily evaluate the degrading effects of finite amount of entanglement, decoherence due to losses, and imperfect detection at receiver's location.

The paper is structured as follows. In Sec. II, we establish notation and describe the general measurement scheme we are going to consider. In Sec. III, we consider the three above detection schemes as conditional measurements to engineer nonclassical states. In Sec. IV, we show how to evaluate detection probabilities and conditional states using Wigner functions. This approach allows us to analyze several degrading effects in CV teleportation, and to show the equivalence of noisy teleportation to a Gaussian noisy channel. Section V closes the paper with some concluding remarks.

II. CONDITIONAL QUANTUM-STATE ENGINEERING

The general measurement scheme we are going to consider is schematically depicted in Fig. 1. The first stage consists of a nondegenerate optical parametric amplifier (NOPA) obtained by a $\chi^{(2)}$ nonlinear optical crystal cut either for type I or type II phase matching. In the parametric approximation (i.e., pump remaining Poissonian during the evolution [29]), the crystal couples two modes of the radiation field according to the effective Hamiltonian

$$H_{\kappa}=\kappa(a^{\dagger}b^{\dagger}+ab), \tag{1}$$

where κ represents the effective nonlinear coupling, sometimes referred to as the *gain* of the amplifier, and a and b denote modes with wave vectors satisfying the phase-matching condition $\vec{k}_a+\vec{k}_b=\vec{k}_p$, $\vec{k}_p$ being the wave vector of the pump. For vacuum input we have parametric down-conversion with the output given by the so-called twin-beam state of radiation,

$$|\lambda\rangle\rangle=\sqrt{1-|\lambda|^2}\sum_{p=0}^{\infty}\lambda^p|pp\rangle\rangle \quad |pp\rangle\rangle=|p\rangle_a\otimes|p\rangle_b, \tag{2}$$

where $\lambda=\tanh|\kappa|\tau$ and τ represents an effective interaction time. The TWB $|\lambda\rangle\rangle$ is an entangled state in the bipartite Hilbert space $\mathcal{H}_a\otimes\mathcal{H}_b$, where $\mathcal{H}_j$, $j=a,b$, are the Fock space of the two modes, respectively.

TWBs are pure states and therefore their degree of entanglement can be quantified by the excess von Neumann entropy $\Delta S=\frac{1}{2}(S[\varrho_a]+S[\varrho_b]-S[\varrho])$ [23–26]. The entropy of a two-mode state ϱ is defined as $S[\varrho]=-\mathrm{Tr}\{\varrho\ln\varrho\}$, whereas the entropies of the two modes a and b are given by $S[\varrho_j]=-\mathrm{Tr}_j\{\varrho_j\ln\varrho_j\}$, $j=a,b$, with $\varrho_a=\mathrm{Tr}_b\{\varrho\}$ and $\varrho_b=\mathrm{Tr}_a\{\varrho\}$ denoting partial traces [27]. The degree of entanglement of the state $|\lambda\rangle\rangle$, in terms of the average number of photons of the TWB $N=2\lambda^2/(1-\lambda^2)$, is given by

$$\Delta S=\ln\left(1+\frac{N}{2}\right)+\frac{N}{2}\ln\left(1+\frac{2}{N}\right). \tag{3}$$

Notice that for pure states, ΔS represents the unique measure of entanglement [28]. TWBs are the maximally entangled states for a given average number of photons, and the degree of entanglement is a monotonically increasing function of N.

A measurement performed on one of the two modes *reduces* the other one according to the projection postulate. Each possible outcome x occurs with probability P_x, and corresponds to a conditional state ϱ_x on the other subsystem. We have

$$\begin{aligned}P_x&=\mathrm{Tr}_{ab}[|\lambda\rangle\rangle\langle\langle\lambda|\mathbb{I}_a\otimes\Pi_x]\\&=(1-\lambda^2)\sum_q\lambda^{2q}\langle q|\Pi_x|q\rangle\\&=(1-\lambda^2)\mathrm{Tr}_b[\lambda^{2b^{\dagger}b}\Pi_x^T],\end{aligned} \tag{4}$$

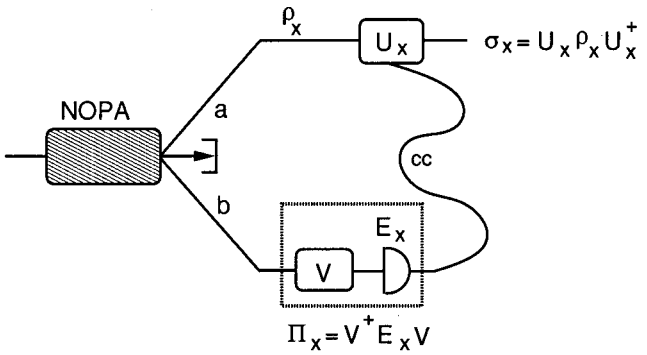

FIG. 1. Scheme for quantum-state engineering assisted by entanglement. At first, a twin beam of the modes a and b is produced by spontaneous down-conversion in a nondegenerate parametric optical amplifier. Then, mode b is (possibly) subjected to the unitary transformation V and then revealed by a measurement apparatus described by the probability operator-valued measure (POVM) E_x. Overall, the quantum operation on the mode b is described by the POVM $\Pi_x=V^{\dagger}E_xV$. The conditional state of mode a is given by ϱ_x, and this state may be further modified by a unitary transformation U_x depending on the outcome of the measurement, whose value may be sent to the receiver location by classical communication. The overall conditional state is thus $\sigma_x=U_x\varrho_xU_x^{\dagger}$. Throughout the paper, we always take $V=\mathbb{I}$ (no transformation before the measurement), and consider three kinds of measurements: on/off photodetection, homodyne detection, and joint measurement of two-mode quadratures by multiport homodyne or heterodyne detection. In the case of on/off photodetection and homodyne detection, we do not consider further transformation (i.e., $U_x=\mathbb{I}$), whereas for the joint measurement of two-mode quadratures, this will a be displacement operator $D(\alpha)$, with amplitude equal to the result of the measurement.

$$\varrho_x = \frac{1}{P_x}\mathrm{Tr}_b[|\lambda\rangle\rangle\langle\langle\lambda|\mathbb{I}_a\otimes\Pi_x] = \frac{1-\lambda^2}{P_x}\sum_{pq}\lambda^{p+q}\langle p|\Pi_x^T|q\rangle|q\rangle\langle p| = \frac{\lambda^{a^\dagger a}\Pi_x^T\lambda^{a^\dagger a}}{\mathrm{Tr}_b[\lambda^{2b^\dagger b}\Pi_x^T]}, \tag{5}$$

where Π_x is the probability operator-valued measure (POVM) describing the measurement, $\{\}^T$ denotes transposition, and $\mathbb{I}_a$ denotes the identity operator on $\mathcal{H}_a$. In the last equalities of both Eqs. (4) and (5), we have already performed the trace over the Hilbert space $\mathcal{H}_a$. Also notice that in the last expression for ϱ_x in Eq. (5), Π_x should be meant as an operator acting on $\mathcal{H}_a$. Our scheme is general enough to include the possibility of performing any unitary operation on the beam subjected to the measurement. In fact, if E_x is the original POVM and V the unitary, the overall measurement process is described by $\Pi_x = V^\dagger E_x V$, which is again a POVM. In the following, we always consider $V=\mathbb{I}$, i.e., no transformation before the measurement. A further generalization consists in sending the result of measurement (by classical communication) to the reduced state location and then performing a conditional unitary operation U_x on the conditional state, eventually leading to the state $\sigma_x = U_x\varrho_x U_x^\dagger$. This degree of freedom will be used in Sec. III C, where we analyze CV quantum teleportation as a conditional measurement.

III. CONDITIONAL MEASUREMENTS ON TWIN BEAM

A. Geiger-like (on/off) photodetection

By looking at the expression (2) of TWB in the Fock basis, it is apparent that ideal photocounting on one of the two beams, described by the POVM $\Pi_n = |n\rangle\langle n|$, is a conditional source of Fock number state $|n\rangle$, which would be produced with a conditional probability $P_n = (1-\lambda^2)\lambda^{2n}$. However, as mentioned above, photocounting cannot be considered a realistic kind of measurement. Therefore, we now consider the situation in which one of the two beams, say mode b, is revealed by an avalanche on/off photodetector, i.e., a detector which has no output when no photon is detected and a fixed output when one or more photons are detected. The action of an on/off detector is described by the two-value POVM $\{\Pi_0,\Pi_1\}$, where

$$\Pi_0 \doteq \sum_{k=0}^{\infty}(1-\eta)^k|k\rangle\langle k|, \quad \Pi_1 \doteq \mathbb{I}-\Pi_0, \tag{6}$$

η being the quantum efficiency. The outcome "1" (i.e., registering a "click" corresponding to one or more incoming photons) occur with probability

$$P_1 = \langle\langle\lambda|\mathbb{I}\otimes\Pi_1|\lambda\rangle\rangle = \frac{\eta\lambda^2}{1-\lambda^2(1-\eta)} = \frac{\eta N}{2+\eta N} \tag{7}$$

and correspondingly, the conditional output states for the mode a is given by

$$\varrho_1 = \frac{1-\lambda^2}{P_1}\sum_{k=1}^{\infty}\lambda^{2k}[1-(1-\eta)^k]|k\rangle\langle k|. \tag{8}$$

The density matrix in Eq. (8) describes a mixture: a *pseudo*-thermal state, where the vacuum component has been removed by the conditional measurement. Such a state is highly nonclassical, as also discussed in Refs. [30,32]. Notice that the nonclassicality is present only when the state exiting the amplifier is entangled. In the limit of low gain, i.e., for small TWB photon number N, the conditional state ϱ_1 approaches the number state $|1\rangle\langle 1|$ with one photon.

The Wigner function of ϱ_1

$$W(\alpha) = \int \frac{d^2\gamma}{\pi^2}e^{\bar{\gamma}\alpha-\bar{\alpha}\gamma}\mathrm{Tr}[\varrho_1 D(\gamma)], \tag{9}$$

where $D(\gamma)=\exp[\gamma a^\dagger - \bar{\gamma}a]$ is the displacement operator, exhibits negative values for any value of λ and η. In particular, in the origin of the phase space, we have

$$W(0) = -\frac{2}{\pi}\frac{1}{N+1}\frac{2+\eta N}{2(1+N)-\eta N}. \tag{10}$$

One can see that also the generalized Wigner function for s ordering,

$$W_s(\alpha) = -\frac{2}{\pi s}\int d^2\gamma W_0(\gamma)\exp\left[\frac{2}{s}|\alpha-\gamma|^2\right],$$

shows negative values for $s\in(-1,0)$. In particular, one has

$$W_s(0) = -\frac{2(1+s)(2+\eta N)}{\pi(1+N-s)[2(1+N-s)-\eta N(1+s)]}. \tag{11}$$

A good measure of nonclassicality is given by the lowest index $s^\star$, for which W_s is a well-behaved probability, i.e., regular and positive definite [31]. Equation (11) says that for ϱ_1 we have $s^\star=-1$, that is, ϱ_1 describes a state as nonclassical as a Fock number state.

The Fano factor

$$F = \frac{\langle[b^\dagger b-\langle b^\dagger b\rangle]^2\rangle}{\langle b^\dagger b\rangle}$$

of ϱ_1 is given by

$$F = \frac{1}{2}(2+N)\left(1+\frac{2}{2+N\,\eta}-\frac{4(2+N)}{4+N(4+N\,\eta)}\right). \tag{12}$$

Therefore, we have that the beam b is always sub-Poissonian for (at least) $N<2$. The verification of nonclassicality can be performed, for any value of the gain, by checking the negativity of the Wigner function through quantum homodyne tomography [32], and in the low-gain regime, also by verifying the sub-Poissonian character by measuring the Fano factor via direct noise detection [33,34].

Notice that besides quantum efficiency, i.e., lost photons, the performance of a realistic photodetector may be degraded

by the presence of dark count, i.e., by ''clicks'' that do not correspond to any incoming photon. In order to take into account both these effects, a real photodetector can be modeled as an ideal photodetector (unit quantum efficiency, no dark count) preceded by a beam splitter (of transmissivity equal to the quantum efficiency), whose second port is in an auxiliary excited state (e.g., a thermal state, or a random-phase coherent state), which accounts for the background noise (thermal or Poissonian). However, at optical frequencies, the number of dark counts is negligible and we are not going to take into account this effect, which has been analyzed in detail in Ref. [32].

We conclude that conditional on/off photodetection on TWB provides a reliable scheme to check nonclassical light. The nonclassicality, as well as its verification, are robust against amplifier gain and detector efficiency.

B. Homodyne detection

In this section, we consider the kind of conditional state that can be obtained by homodyne detection on one of the two beams exiting the NOPA. We will show that they are squeezed states. We first consider ideal homodyne detection described by the POVM $\Pi_x=|x\rangle\langle x|$, where

$$|x\rangle=\left(\frac{2}{\pi}\right)^{1/4}e^{-x^2}\sum_{n=0}^{\infty}\frac{H_n(\sqrt{2}x)}{\sqrt{n!2^n}}|n\rangle,$$

with $H_n(x)$ denoting the nth Hermite polynomials, is an eigenstate of the quadrature operator $x_b=\frac{1}{2}(b+b^\dagger)$. Then in the second part of the section, we will consider two kinds of imperfections: nonunit quantum efficiency and finite resolution. As we will see, the main effect of the conditional measurement, i.e., the generation of squeezing, holds also for these realistic situations.

The probability of obtaining the outcome x from a homodyne detection on the mode b is obtained from Eq. (4). We have

$$P_x=(1-\lambda)^2\sum_{q=0}^{\infty}\lambda^{2q}|\langle x|q\rangle|^2=\frac{\exp\left\{-\frac{x^2}{2\sigma_\lambda^2}\right\}}{\sqrt{2\pi\sigma_\lambda^2}},\quad(13)$$

where

$$\sigma_\lambda^2=\frac{1}{4}\frac{1+\lambda^2}{1-\lambda^2}=\frac{1}{4}(1+N).\quad(14)$$

P_x is Gaussian with variance that increases as λ is approaching unit. In the (unphysical) limit $\lambda\to1$, i.e., infinite gain of the amplifier, the distribution for x is uniform over the real axis. The conditional output state is given by Eq. (5), and since Π_x is a pure POVM, it is a pure state $\varrho_x=|\psi_x\rangle\langle\psi_x|$, where

$$|\psi_x\rangle=\sqrt{\frac{1-\lambda^2}{P_x}}\lambda^{a^\dagger a}|x\rangle=\sum_k\psi_k|k\rangle.\quad(15)$$

The coefficients of $|\psi_x\rangle$ in the Fock basis are given by

$$\psi_k=\left(\frac{\lambda^2}{2}\right)^{k/2}\frac{1}{\sqrt{k!}}(1-\lambda^4)^{1/4}e^{-2\lambda^2x^2/(1+\lambda^2)}H_k(\sqrt{2}x),\quad(16)$$

which means that $|\psi_x\rangle$ is a squeezed state of the form

$$|\psi_x\rangle=D(\alpha_x)S(\zeta)|0\rangle,\quad(17)$$

where

$$\alpha_x=\frac{2x\lambda}{1+\lambda^2}=\frac{x\sqrt{N(N+2)}}{1+N},$$
$$\zeta=\operatorname{arctanh}\lambda^2=\operatorname{arctanh}\frac{N}{N+2}.\quad(18)$$

The quadrature fluctuations are given by

$$\overline{\Delta x_a^2}=\frac{1}{4}\frac{1}{1+N},\quad\overline{\Delta y_a^2}=\frac{1}{4}(1+N),\quad(19)$$

where $x_a=\frac{1}{2}(a^\dagger+a)$, $y_a=(i/2)(a^\dagger-a)$, and $\overline{\Delta O^2}=\mathrm{Tr}[\varrho O^2]-(\mathrm{Tr}[\varrho O])^2$. Equation (19) confirms that $|\psi_x\rangle$ is a minimum uncertainty state. Notice that (i) the amount of squeezing is independent of the outcome of the measurement, which only influences the coherent amplitude; (ii) according to Eq. (13), the most probable conditional state is a squeezed vacuum. The average number of photon of the conditional state is given by

$$N_x=\langle\psi_x|a^\dagger a|\psi_x\rangle=x^2\frac{N(N+2)}{(1+N)^2}+\frac{1}{4}\frac{N^2}{1+N}.\quad(20)$$

The conservation of energy may be explicitly checked by averaging over the possible outcomes,

$$\int dx P_x N_x=\frac{1}{4}\frac{N^2}{1+N}+\sigma_\lambda^2\frac{N(N+2)}{(1+N)^2}=\frac{N}{2},\quad(21)$$

which correctly reproduces the number of photon pertaining each part of the TWB.

We now take into account the effects of nonunit quantum efficiency at the homodyne detector on the conditional state. We anticipate that $\varrho_{x\eta}$ will be no longer pure states, and in particular, they will not be squeezed states of the form (17). Nevertheless, the conditional output states still exhibit squeezing, i.e., quadrature fluctuations below the coherent level, for any value of the outcome x, and for quantum efficiency larger than $\eta>1/2$.

The POVM of a homodyne detector with quantum efficiency η is given by

$$\Pi_{x\eta}=\int\frac{dt}{\sqrt{2\pi\Delta_\eta^2}}\exp\left\{-\frac{(x-t)^2}{2\Delta_\eta^2}\right\}\Pi_t,\quad(22)$$

where

$$\Delta_\eta^2=\frac{1-\eta}{4\eta}.\quad(23)$$

The nonideal POVM is a Gaussian convolution of the ideal POVM. The main effect is that $\Pi_{x\eta}$ is no longer a pure orthogonal POVM. The probability $P_{x\eta}$ of obtaining the outcome x is still a Gaussian, now with variance

$$\Delta^2_{\lambda\eta}=\sigma^2_\lambda+\Delta^2_\eta. \tag{24}$$

The conditional output state is again given by Eq. (5). After some algebra, we get the matrix element in the Fock basis

$$\begin{aligned}\langle n|\varrho_{x\eta}|m\rangle=&\frac{(1-\lambda^2)\lambda^{n+m}}{\sqrt{n!m!2^{n+m}}}\sqrt{\eta\frac{2-\eta(1-\lambda^2)}{1-\lambda^2}}\\&\times\exp\left\{-4x^2\frac{\eta^2\lambda^2}{1-\lambda^2(1-2\eta)}\right\}\\&\times\sum_{k=0}^{min(m,n)}2^k k!\binom{m}{k}\binom{n}{k}\eta^{(m+n)/2-k}\\&\times H_{m+n-2k}(\sqrt{2\eta}x).\end{aligned} \tag{25}$$

The quadrature fluctuations are now given by

$$\overline{\Delta x_a^2}=\frac{1+N(1-\eta)}{4(1+\eta N)},\quad \overline{\Delta y_a^2}=\frac{1}{4}(1+N). \tag{26}$$

As a matter of fact, $\overline{\Delta y_a^2}$ is independent of η, whereas $\overline{\Delta x_a^2}$ increases for decreasing η. Therefore, the conditional output $\varrho_{x\eta}$ is no longer a minimum uncertainty state. However, for η large enough, we still observe squeezing in the direction individuated by the measured quadrature. The form of the output state can be obtained by the explicit calculation of the matrix elements or, more conveniently, by evaluating the Wigner function (see Sec. IV). We have

$$\varrho_{x\eta}=D(\alpha_{x\eta})S(\zeta_\eta)\nu_{th}S^\dagger(\zeta_\eta)D^\dagger(\alpha_{x\eta}), \tag{27}$$

where

$$\nu_{th}=(1+n_{th})^{-1}\sum_{p=0}^{\infty}\left(\frac{n_{th}}{1+n_{th}}\right)^p|p\rangle\langle p|$$

is a thermal state with average number of photons given by

$$n_{th}=\frac{1}{2}\left\{\sqrt{\frac{(1+N)[1+N(1-\eta)]}{1+\eta N}}-1\right\}, \tag{28}$$

and the amplitude and squeezing parameters read as follows:

$$\alpha_{x\eta}=\frac{\eta\sqrt{N(N+2)}}{1+\eta N}x, \tag{29}$$

$$\zeta_\eta=\frac{1}{4}\ln\frac{(1+N)(1+\eta N)}{1+N(1-\eta)}. \tag{30}$$

From Eqs. (26) and (30), we notice that $\varrho_{x\eta}$ shows squeezing if $\eta>1/2$, independent of the actual value x of the homodyne outcome. In Fig. 2, we illustrate the effects of quantum efficiency on the matrix elements of the conditional state. In particular, we plot the matrix elements for two values of the homodyne outcome $x=0.0,0.6$, and three values of the quantum efficiency $\eta=1.0,0.8,0.4$.

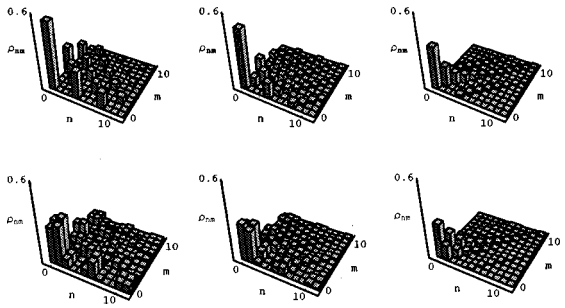

FIG. 2. Matrix elements in the Fock basis of the conditional state $\varrho_{x\eta}$ after homodyne detection on TWB. In the first row, the matrix elements for $x=0.0$ and $\eta=1.0,0.8,0.4$. In the second row, the matrix elements for $x=0.6$ and the same values of quantum efficiency.

The outcome of homodyne detection is, in principle, continuously distributed over the real axis. However, in practice, one has always to discretize data, mostly because of finite experimental resolution. The POVM describing homodyne detection with binned data is given by

$$\Pi_{x\eta}(\delta)=\frac{1}{\delta}\int_{x-\delta/2}^{x+\delta/2}dt\Pi_{t\eta}, \tag{31}$$

where $\Pi_{t\eta}$ is given in Eq. (22), and δ is the width of the bins. The probability distribution is now given by

$$\begin{aligned}P_{x\eta}(\delta)=&\frac{1}{2\delta}\left[\operatorname{erf}\left(\frac{x+\frac{\delta}{2}}{\sqrt{2\Delta^2_{\lambda\eta}}}\right)-\operatorname{erf}\left(\frac{x-\frac{\delta}{2}}{\sqrt{2\Delta^2_{\lambda\eta}}}\right)\right]\\=&\frac{\exp\left\{-\frac{x^2}{2\Delta^2_{\lambda\eta}}\right\}}{\sqrt{2\pi\Delta^2_{\lambda\eta}}}\left\{1-\frac{x^2-\Delta^2_{\lambda\eta}}{24\Delta^2_{\lambda\eta}}\delta^2\right\}+O(\delta^3),\end{aligned} \tag{32}$$

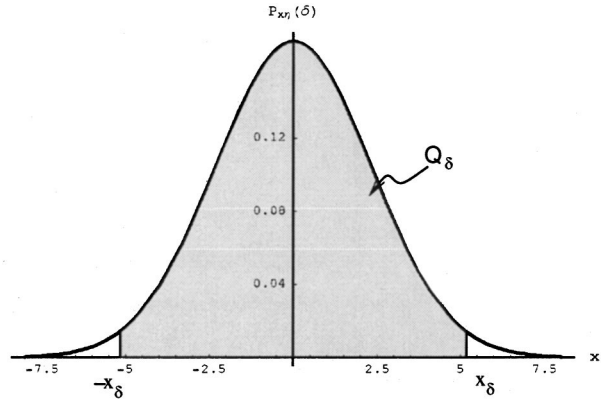

FIG. 3. Probability distribution $P_{x\eta}(\delta)$ of homodyne outcomes x for quantum efficiency $\eta=0.7$, TWB photon number $N=20$, and width of the bins $\delta=0.25$. The threshold value $x_\delta\simeq 5.16$ to obtain a conditionally squeezed state is shown. The gray-shaded area represents the overall probability $Q_\delta\simeq 97\%$ of producing a squeezed state by the conditional measurement.

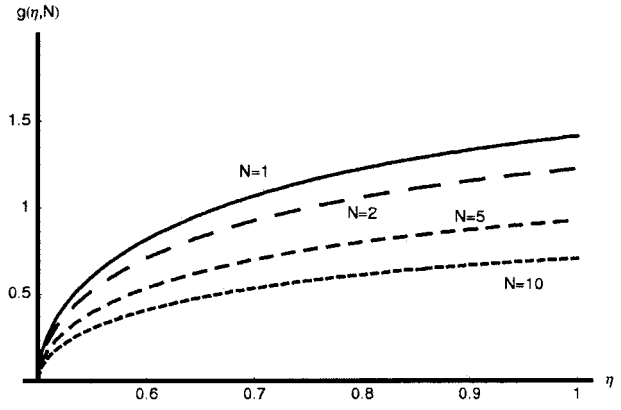

FIG. 4. The function $g(\eta,N)$ in Eq. (36) vs the quantum efficiency for different values of the TWB photon number N. From top to bottom, we have the curves for $N=1,2,5,10$.

where $\Delta^2_{\lambda\eta}$ is given in Eq. (24) and

$$\mathrm{erf}(x)=2/\sqrt{\pi}\int_0^x dt\,\exp\{-t^2\}$$

denotes the error function. The conditional state is modified accordingly. Concerning the quadrature fluctuations of the conditional state, we have, up to second order in δ,

$$\overline{\Delta x_a^2}(\delta)=\overline{\Delta x_a^2}+x^2\frac{\delta^2}{12}\frac{\eta^2N(N+2)}{(1+\eta N)^2}, \tag{33}$$

which is below the coherent level for $\eta>1/2$ and for

$$|x|<x_\delta\equiv\frac{1}{\delta}\sqrt{\frac{3(1+\eta N)(2\eta-1)}{\eta^2(N+2)}}. \tag{34}$$

Therefore, the effect of finite resolution is that the conditional output is squeezed only for the subset $|x|<x_\delta$ of the possible outcomes which, however, represents the range where the probability is higher. In Fig. 3, as an example, we show $P_{x\eta}(\delta)$ as a function of x for $\eta=0.7$, $\delta=0.25$, and $N=20$. The threshold x_δ is shown as well as the overall probability Q_δ of producing a squeezed state which, up to second order in δ, is given by

$$Q_\delta=\int_{-x_\delta}^{x_\delta}dx P_{x\eta}(\delta)=\begin{cases}0, & N=0\\ \mathrm{erf}\left[\dfrac{1}{\delta}g(\eta,N)\right], & N\neq 0,\end{cases} \tag{35}$$

where

$$g(\eta,N)=\sqrt{\frac{6(2\eta-1)}{\eta(N+2)}}. \tag{36}$$

In Fig. 4, we show $g(\eta,N)$ as a function of η for different values of the TWB photon number N. As it is apparent from the plot, $g(\eta,N)$ is a monotonically increasing function of η and a monotonically decreasing function of N. Notice that the larger $g(\eta,N)$ is, the smaller is the effect of finite resolution in decreasing the probability for obtaining squeezed states. In principle, using small value of N (i.e., less entanglement) increases the probability of getting squeezed states. However, such states would be only slightly squeezed, i.e., $\overline{\Delta x_a^2}\lesssim\frac{1}{4}$. Therefore, since the scheme is aimed to be a tunable source of squeezing, the best strategy is to use large values of N, while accepting a slightly decreased conditional probability.

C. Joint measurement of two-mode quadratures

In this section, we assume that mode b is subjected to the measurement of the real and the imaginary part of the complex operator $Z=b+c^\dagger$, where c is an additional mode excited in a reference state S. The measurements of Re$[Z]$ and Im$[Z]$ correspond to measuring the sum and difference quadratures x_b+x_c and y_b-y_c of the two modes, and can be experimentally implemented by multiport homodyne detection if the two modes have the same frequencies [35–37], or by heterodyne detection otherwise [38]. The measurement is described by the following POVM [39]:

$$\Pi_\alpha=\frac{1}{\pi}D(\alpha)S^TD^T(\alpha), \tag{37}$$

where α is a complex number, $D(\alpha)$ is the displacement operator, and $(\cdots)^T$ stands for the transposition operation. The present scheme is equivalent to that of CV teleportation, which can be viewed as a conditional measurement, with the state to be teleported playing the role of the reference state S of the apparatus. In order to complete the analogy, we assume that the result of the measurement is classically transmitted to the receiver's location, and that a displacement operation $D^\dagger(\alpha)$ is performed on the conditional state ϱ_α. Equations (4) and (5) are rewritten as

$$p_\alpha=(1-\lambda^2)\mathrm{Tr}^2[\lambda^{2a^\dagger a}\Pi_\alpha^T], \tag{38}$$

$$\varrho_\alpha=\frac{\lambda^{a^\dagger a}\Pi_\alpha^T\lambda^{a^\dagger a}}{\mathrm{Tr}^2[\lambda^{2a^\dagger a}\Pi_\alpha^T]}, \tag{39}$$

$$\sigma_\alpha=D^T(\alpha)\varrho_\alpha D(\alpha), \tag{40}$$

while the teleported state is the average over all the possible outcomes, i.e.,

$$\sigma=\int d^2\alpha p_\alpha\sigma_\alpha=\int d^2\alpha D^\dagger(\alpha)\langle\langle\lambda|\mathbb{I}\otimes\Pi_\alpha|\lambda\rangle\rangle D(\alpha). \tag{41}$$

After performing the partial trace, and some algebra, one has

$$\sigma=\int\frac{d^2\alpha}{\pi K_0}\exp\left\{-\frac{|\alpha|^2}{K_0}\right\}D(\alpha)SD^T(\alpha), \tag{42}$$

where $K_0=1+N-\sqrt{N(N+2)}$. The output state ϱ coincides with the input only in the limit $N\to\infty$, i.e., for infinite energy of the TWB. Equation (42) shows that CV teleportation with finite amount of entanglement is equivalent to a Gaussian displacement channel with K_0 background photons applied to the input state. This result has been also obtained in Refs. [40,41] by different methods. In the following section, we will show that this result still holds taking into account the

effects of decoherence due to losses, and nonunit quantum efficiency of the measurement, either multiport homodyne or heterodyne detection.

IV. CONDITIONAL MEASUREMENTS IN THE PHASE SPACE

The results of the previous sections can be derived, and for CV teleportation also extended, using Wigner functions in the phase space. The analysis is based on the fact that the trace between two operators can be written as [43]

$$\mathrm{Tr}[O_1 O_2] = \pi \int d^2\beta W[O_1](\beta) W[O_2](\beta), \tag{43}$$

where the Wigner function for a generic operator O is defined analogously to that of a density matrix, i.e.,

$$W[O](\alpha) = \int \frac{d^2\gamma}{\pi^2} e^{\alpha\bar{\gamma} - \bar{\alpha}\gamma} \mathrm{Tr}[OD(\gamma)], \tag{44}$$

where α is a complex number and $D(\gamma)$ is the displacement operator. The inverse transformation reads as follows [42]:

$$O = \int d^2\alpha W[O](\alpha) e^{-2|\alpha|^2} e^{2\alpha a^\dagger} (-1)^{a^\dagger a} e^{2\bar{\alpha} a}. \tag{45}$$

The Wigner function $W[\lambda](x_1,y_1;x_2,y_2)$ of a TWB is Gaussian (we omit the argument):

$$W[\lambda] = (2\pi\sigma_+^2 2\pi\sigma_-^2)^{-1} \exp\left[-\frac{(x_1+x_2)^2}{4\sigma_+^2} - \frac{(y_1+y_2)^2}{4\sigma_-^2} - \frac{(x_1-x_2)^2}{4\sigma_-^2} - \frac{(y_1-y_2)^2}{4\sigma_+^2} \right], \tag{46}$$

where the variances are given by

$$\sigma_+^2 = \frac{1}{4}[1+N+\sqrt{N(N+2)}], \tag{47}$$

$$\sigma_-^2 = \frac{1}{4}[1+N-\sqrt{N(N+2)}]. \tag{48}$$

Using Eq. (43), we rewrite the probability distribution (4) as follows:

$$P_x = \int\int dx_1 dy_1 \int\int dx_2 dy_2 W[\lambda](x_1,y_1;x_2,y_2) \times W[\Pi_x](x_2,y_2) \tag{49}$$

$$= (1-\lambda^2) \int\int dx_2 dy_2 W[\lambda^{2b^\dagger b}](x_2,y_2) W[\Pi_x](x_2,y_2), \tag{50}$$

where $W[\Pi_x](x_2,y_2)$ is the Wigner function of the POVM describing the measurement and $W[\lambda^{2b^\dagger b}]$ is given by

$$W[\lambda^{2b^\dagger b}](x_2,y_2) = \frac{1}{\pi(1+N)} \exp\left(-\frac{x_2^2+y_2^2}{1+N} \right). \tag{51}$$

Analogously, the Wigner function of the conditional output state (5) can be written as

$$W[\varrho_x](x_1,y_1) = \frac{1}{P_x} \int\int dx_2 dy_2 W[\lambda](x_1,y_1;x_2,y_2) \times W[\Pi_x](x_2,y_2). \tag{52}$$

Once the Wigner function for the POVM Π_x of the detector is known, one may reproduce the results of previous sections using Eqs. (50) and (52) together with Eq. (45). For on/off photodetection, one has

$$W[\Pi_0](x_2,y_2) = \frac{2\eta}{\pi(2-\eta)} \exp\left(-2\frac{x_2^2+y_2^2}{2-\eta} \right),$$

$$W[\Pi_1](x_2,y_2) = 1 - W[\Pi_0](x_2,y_2), \tag{53}$$

whereas the POVM of a homodyne detector with quantum efficiency η corresponds to the Wigner function given by

$$W[\Pi_{x\eta}](x_1,y_1) \equiv W[\Pi_{x\eta}](x_1) = (2\pi\Delta_\eta^2)^{-1/2} \exp\left\{ -\frac{(x_1-x)^2}{2\Delta_\eta^2} \right\}, \tag{54}$$

where Δ_η^2 is given in Eq. (23).

Let us now focus our attention on the situation where the conditional measurement on TWB is the joint measurement of the sum and difference quadratures of two modes. In this case, the Wigner approach may be convenient, in particular, in the description of optical teleportation as a conditional measurement, since it makes it easier to include the degrading effects of nonunit quantum efficiency and of losses along the transmission channel.

At first, we consider the ideal POVM Π_α of Eq. (37). By taking into account that for any density matrix

$$W[\varrho^T](x,y) = W[\varrho](x,-y),$$

$$W[D(\alpha)\varrho D^\dagger(\alpha)](x,y) = W[\varrho](x-x_\alpha, y-y_\alpha), \tag{55}$$

with $x_\alpha = \mathrm{Re}[\alpha]$ and $y_\alpha = \mathrm{Im}[\alpha]$, it is easy to show that

$$W[\Pi_\alpha^T](x_2,y_2) = W[S](x_2-x_\alpha, y_\alpha - y_2). \tag{56}$$

Inserting Eq. (56) in Eqs. (50) and (52), and changing the integration variables, we obtain the Wigner function of the teleported state σ of Eq. (40):

$$W[\sigma](x_2,y_2) = \int\int dx_1 dy_1 \int\int dx_\alpha dy_\alpha W[\lambda](x_2+x_\alpha, y_2 + y_\alpha; x_1+x_\alpha, -y_1-y_\alpha) W[S](x_1,y_1)$$

$$= \int\int \frac{dx_1 dy_1}{\pi K_0} \exp\left\{ -\frac{x_1^2+y_1^2}{K_0} \right\} \times W[S](x_2-x_1, y_2-y_1), \tag{57}$$

which corresponds to the state given by Eq. (42). We now proceed by taking into account nonunit quantum efficiency of the detector and losses due to propagation of TWB. Nonunit quantum efficiency at either double homodyne or heterodyne detectors modifies the POVM of the sender, which becomes a Gaussian convolution of the ideal POVM Π_α,

$$\Pi_{\alpha\eta}=\int \frac{d^2\beta}{\pi D_\eta^2}\exp\left\{-\frac{|\alpha-\beta|^2}{D_\eta^2}\right\}\Pi_\beta, \quad D_\eta^2=\frac{1-\eta}{\eta}, \tag{58}$$

leading to

$$W[\Pi_{\alpha\eta}](x_2,y_2)=\int\int \frac{dx_\beta dy_\beta}{\pi D_\eta^2}\exp\left(-\frac{x_\beta^2+y_\beta^2}{D_\eta^2}\right) \times W[S](x_\beta+x_2-x_\alpha, y_\alpha-y_2-y_\beta). \tag{59}$$

On the other hand, losses that may occur during the propagation of TWB degrade the entanglement. This effect can be described as the coupling of each part of the TWB with a nonzero temperature reservoir. The dynamics is described by the two-mode master equation,

$$\frac{dR_t}{dt}\equiv \mathcal{L}R_t=\Gamma(1+M)L[a]R_t+\Gamma(1+M)L[b]R_t +\Gamma M L[a^\dagger]R_t+\Gamma M L[b^\dagger]R_t, \tag{60}$$

where $R_t\equiv R(t)$, $R_0=|x\rangle\rangle\langle\langle x|$, Γ denotes the (equal) damping rate, M the number of background thermal photons, and $L[O]$ is the Lindblad superoperator $L[O]R_t=OR_tO^\dagger-\frac{1}{2}O^\dagger OR_t-\frac{1}{2}R_tO^\dagger O$. The terms proportional to $L[a]$ and $L[b]$ describe the losses, whereas the terms proportional to $L[a^\dagger]$ and $L[b^\dagger]$ describe a linear phase-insensitive amplification process. This can be due to either optical media dynamics or thermal hopping; in both cases, no phase information is carried. Of course, the dissipative dynamics of the two channels are independent of each other. The master equation (60) can be transformed into a Fokker-Planck equation for the two-mode Wigner function of the TWB. Using the differential representation of the superoperators in Eq. (60), the corresponding Fokker-Planck equation reads as follows:

$$\partial_\tau W_\tau=\left[\frac{1}{8}\left(\sum_{j=1}^{2}\partial^2_{x_jx_j}+\partial^2_{y_jy_j}\right)+\frac{\gamma}{2}\left(\sum_{j=1}^{2}\partial_{x_j}x_j+\partial_{y_j}y_j\right)\right]W_\tau, \tag{61}$$

where τ denotes the rescaled time $\tau=\Gamma/\gamma t$, and $\gamma=(2M+1)^{-1}$ the drift term. The solution of Eq. (61) can be written as

$$W_\tau=\int dx_1'\int dx_2'\int dy_1'\int dy_2' W[\lambda](x_1',y_1';x_2',y_2') \times\prod_{j=1}^{2}G_\tau(x_j|x_j')G_\tau(y_j|y_j'), \tag{62}$$

where $W[\lambda]$ is initial Wigner function of the TWB, and the Green functions $G_\tau(x_j|x_j')$ are given by

$$G_\tau(x_j|x_j')=\frac{1}{\sqrt{2\pi D^2}}\exp\left[-\frac{(x_j-x_j'e^{-(1/2)\gamma\tau})^2}{2D^2}\right],$$

$$D^2=\frac{1}{4\gamma}(1-e^{-\gamma\tau}). \tag{63}$$

The Wigner function W_τ can be obtained by the convolution (62), which can be easily evaluated since the initial Wigner function is Gaussian. The form of W_τ is the same of $W[\lambda]$ with the variances changed to

$$\sigma_+^2\to(e^{-\gamma\tau}\sigma_+^2+D^2),$$

$$\sigma_-^2\to(e^{-\gamma\tau}\sigma_-^2+D^2). \tag{64}$$

Inserting the Wigner functions of the POVM $\Pi_{\alpha\eta}$ and of the evolved TWB in Eq. (52), we obtain the teleported state in the general case. This still has the form (42), however with the parameter K now given by

$$K=K_0e^{-\Gamma t}+(2M+1)(1-e^{-\Gamma t})+D_\eta^2. \tag{65}$$

Equations (42) and (65) summarize the possible effects that degrade the quality of teleportation. In the special case of coherent-state teleportation, one has $S=|z\rangle\langle z|$, which corresponds to original optical CV teleportation experiments [20]. The fidelity $F=\langle z|\sigma|z\rangle$ can be evaluated straightforwardly as the overlap of the Wigner functions. Since $W[z](\alpha)=(2/\pi)e^{-2|\alpha-z|^2}$ is the Wigner function of a coherent state, we have

$$F=\frac{1}{1+K_0e^{-\Gamma t}+(1-e^{-\Gamma t})(2M+1)+(1-\eta)/\eta}.$$

In order to verify quantum teleportation, i.e., to show that the scheme is a truly nonlocal protocol, the fidelity should fulfill the bound $F>1/2$ [20], i.e.,

$$K_0e^{-\Gamma t}+(1-e^{-\Gamma t})(2M+1)+(1-\eta)/\eta<1.$$

Therefore, given the value of the parameters Γ, M, and η in order to verify quantum teleportation, one should use TWB with an average number of photons large enough to satisfy the inequality

$$K_0<e^{\Gamma t}\left[2-\frac{1}{\eta}-(2M+1)(1-e^{-\Gamma t})\right], \tag{66}$$

where, for large N, $K_0=1+N-\sqrt{N(N+2)}$ decreases as $(2N)^{-1}$.

V. SUMMARY AND CONCLUSIONS

A measurement performed on one beam of a TWB reduces the other one according to the projection postulate. This effect is an intrinsic quantum mechanism to achieve effective nonlinear dynamics. We have analyzed in detail the use of conditional measurement on TWB to generate and manipulate quantum states of light. In particular, we have studied realistic measurement schemes taking into account imperfections of the apparatuses, such as detection quantum efficiency and finite resolution.

The first kind of measurement we have analyzed is on/off photodetection which provides a reliable scheme to check nonclassical light. The nonclassicality and its verification are robust against the TWB energy and the detector efficiency. The second apparatus is a homodyne detector, whose action on TWB represents a tunable source of squeezed light, with high conditional probability and robustness to experimental imperfections. In particular, in the ideal case, the conditional output state is a pure minimum uncertainty state with two features: the amount of squeezing is independent of the outcome of the measurement, which only influences the coherent amplitude, and the most probable conditional state is a squeezed vacuum. Taking into account the effect of nonunit quantum efficiency and finite resolution, we have that the conditional state is no longer a pure state, however, still showing squeezing for quantum efficiency larger than $\eta = 1/2$ and for a large range of the homodyne outcomes.

Finally, we have shown how to describe optical CV teleportation as a conditional measurement of the sum and difference quadratures of two modes. We found that realistic CV teleportation with finite amount of entanglement is equivalent to a Gaussian channel with $K_0 \simeq (2N)^{-1}$ background photons applied to the input state, N being the average photon number of the TWB. Using Wigner functions we have also shown that the teleportation in the general case, i.e., taking into account the degrading effects of finite amount of entanglement, decoherence due to losses, and imperfect detection, still corresponds to a Gaussian channel, however with an increased number of background photons [see Eq. (65)]. A bound on the average TWB energy, in order to verify quantum teleportation of coherent states, has been derived.

We conclude that performing conditional measurements on entangled twin beam is a powerful and robust method of engineering nonclassical states of light.

ACKNOWLEDGMENTS

This work has been sponsored by the INFM through the Project No. PRA-2002-CLON and by MIUR through the PRIN projects ''Entanglement Assisted High Precision Measurements and Decoherence Control in Quantum Information Processing.''

[1] Proceedings of Conference on Quantum Interferometry III, edited by F. De Martini, G. Denardo, and L. Hardy, special issue of Fortschr. Phys. **48**(5-7) (2000); Proceedings of Conference on Quantum Interferometry IV, edited by F. De Martini, special issue of Fortschr. Phys. **51**(4-5) (2003).

[2] *Quantum Communication, Computing, and Measurement II*, edited by P. Kumar, G. M. D'Ariano, and O. Hirota (Kluwer Academic, Dordrecht, 2000); *Quantum Communication, Computing, and Measurements III*, edited by P. Tombesi and O. Hirota (Kluwer, Dordrecht, 2001).

[3] J. von Neumann, *Mathematical Foundations of Quantum Mechanics* (Princeton University Press, Princeton, NJ, 1955), pp. 442–445.

[4] G.M. D'Ariano, P. Kumar, Macchiavello, L. Maccone, and N. Sterpi, Phys. Rev. Lett. **83**, 2490 (1999).

[5] T. Opatrný, G. Kurizki, and D.-G. Welsch, Phys. Rev. A **61**, 032302 (2000); M. Dakna *et al.*, Opt. Commun. **145**, 309 (1998).

[6] D.T. Pegg, L.S. Philips, and S.M. Barnett, Phys. Rev. Lett. **81**, 1604 (1998).

[7] M. Dakna *et al.*, Phys. Rev. A **55**, 3184 (1997).

[8] M. Dakna *et al.*, Acta Phys. Slov. **48**, 207 (1998).

[9] S.B. Zheng, Phys. Lett. A **245**, 11 (1998).

[10] G.M. D'Ariano, L. Maccone, M.G.A. Paris, and M.F. Sacchi, Phys. Rev. A **61**, 053817 (2000); Fortschr Phys. **48**, 511 (2000)

[11] Lu-Ming Duan, G. Giedke, J.I. Cirac, and P. Zoller, Phys. Rev. Lett. **84**, 4002 (2000).

[12] B. Hladky, G. Drobny, and V. Buzek, Phys. Rev. A **61**, 022102 (2000).

[13] M.G.A. Paris, Phys. Rev. A **62**, 033813 (2000).

[14] J. Clausen *et al.*, J. Opt. B: Quantum Semiclassical Opt. **1**, 332 (1999).

[15] A. Napoli, A. Messina, and S. Maniscalco, Acta Phys. Slov. **50**, 519 (2000).

[16] F. Plastina and F. Piperno, Eur. Phys. J. D **5**, 411 (1999).

[17] M. Ban, Opt. Commun. **143**, 225 (1997).

[18] A. Kozhekin, G. Kurizky, and B. Sherman, Phys. Rev. A **54**, 3535 (1996).

[19] O. Aytur and P. Kumar, Phys. Rev. Lett. **65**, 1551 (1990).

[20] A. Furusawa *et al.*, Science **282**, 706 (1998).

[21] M.G.A. Paris, Phys. Lett. A **225**, 28 (1997).

[22] D. James and P. Kwiat, Phys. Rev. Lett. **89**, 183601 (2002).

[23] S.M. Barnett and S.J.D. Phoenix, Phys. Rev. A **44**, 535 (1991).

[24] G. Lindblad, Commun. Math. Phys. **33**, 305 (1973).

[25] S.M. Barnett and S.J.D. Phoenix, Phys. Rev. A **40**, 2404 (1989).

[26] V. Vedral, M.B. Plenio, K. Jacobs, and P.L. Knight, Phys. Rev. A **56**, 4452 (1997).

[27] H. Araki and E.H. Lieb, Commun. Math. Phys. **18**, 160 (1970).

[28] S. Popescu and D. Rohrlich, Phys. Rev. A **56**, R3319 (1997).

[29] G.M. D'Ariano, M.G.A. Paris, and M.F. Sacchi, Nuovo Cimento B **114**, 339 (1999).

[30] L. Mandel and E. Wolf, *Optical Coherence and Quantum Optics* (Cambridge University Press, Cambridge, England, 1995), p. 625.

[31] C.T. Lee, Phys. Rev. A **44**, R2775 (1991).

[32] M.G.A. Paris, Phys. Lett. A **289**, 167 (2001).

[33] S. Youn, S. Choi, P. Kumar, and N. Lee, Opt. Lett. **21**, 1597 (1996).
[34] M. Bondani and M.G.A. Paris, J. Opt. B: Quantum Semiclassical Opt. **4**, 426 (2002).
[35] G.M. D'Ariano and M.F. Sacchi, Phys. Rev. A **52**, R4309 (1995).
[36] G.M. D'Ariano and M.G.A. Paris, Phys. Rev. A **49**, 3022 (1994).
[37] M.G.A. Paris, A. Chizhov, and O. Steuernagel, Opt. Commun. **134**, 117 (1997).
[38] H. Yuen and J. Shapiro, IEEE Trans. Inf. Theory **IT-26**, 78 (1980).
[39] P. Busch and P.J. Lahti, Riv. Nuovo Cimento **18**, 1 (1995).
[40] H.F. Hofmann *et al.*, Phys. Rev. A **62**, 062304 (2000).
[41] M. Ban *et al.*, e-print quant-ph/0202172.
[42] G.M. D'Ariano and M.F. Sacchi, Nuovo Cimento B **112**, 881 (1997).
[43] K. Cahill and R. Glauber, Phys. Rev. **177**, 1857 (1969).